Available online at www.sciencedirect.com
ScienceDirect
Dyes and Pigments 79 (2008) 159–165
DYES and PIGMENTS
www.elsevier.com/locate/dyepig

The synthesis of aminoazobenzenes and the effect of intermolecular hydrogen bonding on their photoisomerization

Qi Ya [a,b], Xian-Zi Dong [a,b], Wei-Qiang Chen [a,*], Xuan-Ming Duan [a,*]

[a] *Laboratory of Organic NanoPhotonics and Laboratory of Organic Optoelectronic Functional Materials and Molecular Engineering, Technical Institute of Physics and Chemistry, Chinese Academy of Sciences, Zhongguancunbeiyitiao No. 2, Haidian District, Beijing 100080, PR China*
[b] *Graduate School of the Chinese Academy of Sciences, Zhongguancunbeiyitiao No. 2, Beijing 100080, PR China*

Received 6 December 2007; received in revised form 4 February 2008; accepted 5 February 2008
Available online 21 February 2008

Abstract

Two series of azobenzene derivatives were synthesized so as to investigate the effects of intermolecular hydrogen bonding on their photochemistry. Photoisomerization in polymer matrices was investigated under various irradiation conditions using UV pulsed laser light. Rate constants were calculated according to equations for reversible photoisomerization. Although aminoazobenzenes exhibited faster photoisomerization and larger integral rate constants than the corresponding acetylamino derivatives, the latter compounds displayed faster conversion from the *trans* to the *cis* form owing to potential intermolecular hydrogen bonding interaction between the acetylamino groups. Long alkyl chain azobenzenes possessed faster photoisomerization rates than those with short alkyl chains.

Keywords: Azobenzene; Synthesis; Intermolecular hydrogen bonding; Dynamic equilibrium; Photoisomerization; Substitute effect

1. Introduction

In the past years, azo dyes have been attracting intensive interest for their potential use in optical data storage [1], optical switching [2], polarization holography [3,4], optical modulation [5], nonlinear optics [6], and photolabile surfactants [7]. Recently, most works are investigating the photoinduced motions resulting from photoisomerization of the azo moieties, which are connected to the side chain of the polymer or doped into the polymer matrix [8,9].

It is well known that the substituents of azo chromophores play an important role in molecular motion during photoisomerization. Many efforts have been made to investigate the motion of azobenzene derivatives by introducing substituents, such as chloro atom into the 2′-position [1], naphthalene [10,11] or carbazole moiety [12] into the azobenzene chromophore, even extending the chromophore by two azo moieties [13]. According to the classification by Rau [14], azobenzene derivatives can be divided into three groups based on their photochemical behavior. One of these is *aminoazobenzene* group. They possessed longer *cis* lifetimes than ''*pseudostilbene*'' group, although their extinction coefficient is smaller than that of *pseudostilbenes*. Consequently, aminoazobenzenes are also treated as good candidates for photoinduced birefringence materials when a blue or green laser is used as a pump source [14]. Moreover, potential hydrogen bondings in azobenzenes also influence their properties. Intramolecular hydrogen bonding (H-bonding), formed by introducing *o*-hydroxyl phenyl moiety into azobenzene, has significant effect on liquid crystalline properties [15]. It is also reported that azobenzenes with intramolecular H-bonding possess a longer *cis* isomer lifetime and have potential application in photoswitching [16].

Our attention was given to the intermolecular H-bonding effect on the photochemical behavior of aminoazobenzenes. In this paper, two kinds of aminoazobenzene derivatives $\mathbf{I}_{\mathbf{a-c}}$ and $\mathbf{II}_{\mathbf{a-c}}$ were designed and synthesized to understand the

* Corresponding authors. Tel.: +86 10 82543596; fax: +86 10 82543597.
E-mail addresses: chenwq7315@mail.ipc.ac.cn (W.-Q. Chen), xmduan@mail.ipc.ac.cn (X.-M. Duan).

0143-7208/$ - see front matter © 2008 Elsevier Ltd. All rights reserved.
doi:10.1016/j.dyepig.2008.02.004

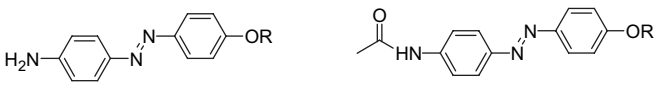

$\mathbf{I_a}$ R = H
$\mathbf{I_b}$ R = $(CH_2)_3OH$
$\mathbf{I_c}$ R = $(CH_2)_6OH$

$\mathbf{II_a}$ R = H
$\mathbf{II_b}$ R = $(CH_2)_3OH$
$\mathbf{II_c}$ R = $(CH_2)_6OH$

Scheme 1. The molecular structures of $\mathbf{I_{a-c}}$ and $\mathbf{II_{a-c}}$.

substituents' effect on the photoisomerization process (Scheme 1). The photoisomerization behaviors of the polymer matrix (PMMA) doped with $\mathbf{I_{a-c}}$ and $\mathbf{II_{a-c}}$ were investigated by varying the irradiating laser power and the doping concentration of azobenzenes. Furthermore, the substituent and concentration effects on the rate constant of photoisomerization are discussed.

2. Experimental detail

2.1. Materials

4-Acetylaminoaniline, phenol, sodium nitrite, hydrochloric acid (36–38%), sodium hydroxide, tetrahydrofuran and chloroform-*d* were purchased from Beijing Chemical and Reagent Company. 3-Chloropropan-1-ol and 6-chlorohexan-1-ol were obtained from J&K Chemicals. All the reagents and solvents were used as-received without further purification.

2.2. Synthesis and characterizations

Compounds $\mathbf{I_{a-c}}$ and $\mathbf{II_{a-c}}$ used in this paper were synthesized according to previously reported procedure [17,18]. ^{1}H NMR spectra were recorded on a Varian Jemini-300/Brucker AV 400 spectrometer using $CDCl_3$ as a solvent and all shifts are referenced to tetramethylsilane (TMS). The fine splitting of phenyl ring patterns is ignored and the signals are reported as simple doublets, with J values referring to the two most intense peaks. Infrared spectra were recorded on an FT/IR-410 spectrophotometer (JASCO Corp.) and mass spectra were measured on a ZAB-HS (Micromass, UK). All data of $\mathbf{I_{a-c}}$ and $\mathbf{II_{a-c}}$ are listed below.

2.2.1. 4-Hydroxy-4′-aminoazobenzene ($\mathbf{I_a}$)

Yield = 96%; m.p. 184–186 °C (lit. [18] m.p. 185–186 °C); ^{1}H NMR (300 MHz, $CDCl_3$, δ ppm): 7.82 (dd, 4H, $J_1 = 9.3$ Hz, $J_2 = 8.7$ Hz), 6.94 (d, 2H, $J = 9.3$ Hz), 6.77 (d, 2H, $J = 8.7$ Hz), 5.04 (s, 1H), 4.02 (s, 2H); IR (KBr, cm^{-1}): 3371, 3284, 1594, 1497, 1470, 1235, 841; HRMS (ESI$^+$) ($M + Na^+$): calcd 236.0794, found: 236.0786 (−3.4 ppm).

2.2.2. 4-Amino-4′-3-hydroxy-propoxyazobenzene ($\mathbf{I_b}$)

Yield = 98%; m.p. 127–129 °C; ^{1}H NMR (300 MHz, $CDCl_3$, δ ppm): 7.86 (d, 2H, $J = 8.8$ Hz), 7.80 (d, 2H, $J = 8.6$ Hz), 7.01 (d, 2H, $J = 8.8$ Hz), 6.76 (d, 2H, $J = 8.6$ Hz), 4.22 (m, 2H), 3.78 (m, 2H), 2.21 (s, 1H), 2.11 (m, 2H); HRMS (ESI$^+$) ($M + Na^+$): calcd 294.1213, found: 294.1230 (+5.8 ppm).

2.2.3. 4-Amino-4′-6-hydroxy-hexyloxyazobenzene ($\mathbf{I_c}$)

Yield = 97%; m.p. 131–133 °C; ^{1}H NMR (400 MHz, $CDCl_3$, δ ppm): 7.84 (d, 2H, $J = 8.9$ Hz), 7.76 (d, 2H, $J = 8.6$ Hz), 6.98 (d, 2H, $J = 8.9$ Hz), 6.75 (d, 2H, $J = 8.6$ Hz), 4.05 (t, 2H, $J = 6.5$ Hz), 3.98 (br s, 2H), 3.70 (m, 2H), 1.87 (m, 2H), 1.66 (m, 2H), 1.56 (s, 1H), 1.53 (m, 2H); HRMS (ESI$^+$) ($M + H^+$): calcd 314.1863, found: 314.1856 (−2.2 ppm).

2.2.4. 4-Hydroxy-4′-acetaminoazobenzene ($\mathbf{II_a}$)

Yield = 88%; m.p. 194–198 °C; ^{1}H NMR (300 MHz, $CDCl_3$, δ ppm): 7.90 (dd, 4H, $J_1 = 8.5$ Hz, $J_2 = 8.6$ Hz), 7.68 (d, 2H, $J = 8.5$ Hz), 6.97 (d, 2H, $J = 8.6$ Hz), 2.24 (s, 3H); IR (KBr, cm^{-1}): 3428, 3325, 1663, 1594, 1551, 1508, 1382, 1266, 847; HRMS (ESI$^+$) ($M + Na^+$): calcd 278.0900, found: 278.0892 (−2.9 ppm).

2.2.5. 4-Acetamino-4′-(3-hydroxypropoxy)azobenzene ($\mathbf{II_b}$)

Yield = 97%; m.p. 178–180 °C; ^{1}H NMR (300 MHz, CD_3OD, δ ppm): 7.86 (m, 4H), 7.72 (d, 2H, $J = 8.8$ Hz), 7.06 (d, 2H, $J = 8.8$ Hz), 4.19 (t, 2H, $J = 6.2$ Hz), 3.78 (t, 2H, $J = 6.2$ Hz), 2.15 (s, 3H), 2.04 (m, 2H); HRMS (ESI$^+$) ($M + Na^+$): calcd 336.1318, found: 336.1308 (−3.0 ppm).

2.2.6. 4-Acetamino-4′-(6-hydroxyhexyloxy)azobenzene ($\mathbf{II_c}$)

Yield = 76%; m.p. 174–175 °C; ^{1}H NMR (300 MHz, CD_3OD, δ ppm): 8.32 (s, 1H), 7.73 (d, 2H, $J = 9.0$ Hz), 7.62 (d, 2H, $J = 8.8$ Hz), 7.05 (d, 2H, $J = 9.0$ Hz), 6.66 (d, 2H, $J = 8.8$ Hz), 4.05 (t, 2H, $J = 6.5$ Hz), 3.42 (m, 2H), 2.54 (s, 3H), 2.09 (s, 1H), 1.75 (m, 2H), 1.46 (m, 6H); HRMS (ESI$^+$) ($M + Na^+$): calcd 378.1788, found: 378.1773 (−4.0 ppm).

2.3. Sample preparation and physical measurements

The $CHCl_3$ solution of azobenzenes **I** and **II** was used for the absorption spectra measurements with a concentration of 5.0×10^{-5} M. All the films used in the photoisomerization experiments were prepared by spin coating a solution onto a cleaned glass slide; the concentration of azobenzenes in solvent ($CHCl_3$ or THF) was 0.01 M. The doped concentration of azobenzenes in PMMA was 10% except for those specially marked. The films were heated at 60 °C for 1 h and allowed to stand in vacuum overnight to remove residual solvent. The IR spectra of the films were recorded on a 3100 FT-IR (Varian).

For the photoisomerization experiments, a laser beam from an Nd:YAG laser was employed as the light source at a wavelength of 355 nm with a pulse width of 8 ns and repetition rate of 10 Hz. The diameter of the laser beam was 1 cm. Photoirradiation was carried out until the photoisomerization reached its photostationary state. The ultraviolet–visible (UV–vis) spectra were recorded by a UV-2550 Shimadzu UV–vis spectrophotometer.

3. Results

3.1. IR spectra

Infrared spectrum presented rich information about the azobenzene-doped PMMA film. As shown in Fig. 1A, $\mathbf{I_b}$ in

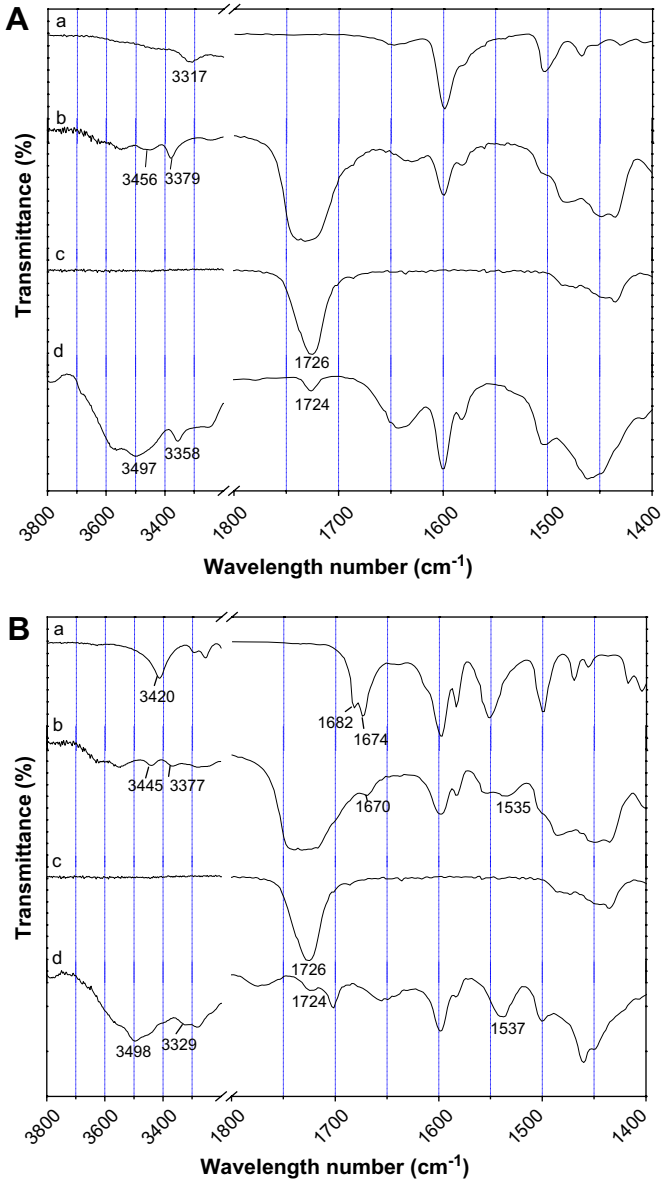

Fig. 1. (A) IR spectra of $\mathbf{I_b}$ in KBr film (a), $\mathbf{I_b}$ in PMMA film (b), PMMA (c) and $\mathbf{I_b}$ (d) in THF solution. (B) IR spectra of $\mathbf{II_b}$ in KBr film (a), $\mathbf{II_b}$ in PMMA film (b), PMMA (c) and $\mathbf{II_b}$ (d) in THF solution.

KBr exhibited the N–H stretching vibration of aggregated amine at 3317 cm^{-1}. The N–H band shifted to 3379 cm^{-1} in PMMA, which indicates the intermolecular H-bonding formation between amino group of $\mathbf{I_b}$ and C=O in PMMA. Similar H-bonding was reported between carbonyl group and hydroxyl group [19]. This H-bonding can be indirectly verified by a similar IR band of $\mathbf{I_b}$ in THF at 3358 cm^{-1} corresponding to N–H···O (THF) stretching. The H-bonding between OH of $\mathbf{I_b}$ and C=O in PMMA appeared at 3456 cm^{-1}, which can be confirmed by the vibration band at 3500 cm^{-1} corresponding to O–H···O (THF) stretching.

When the amino group was converted into an acetylamino group, two kinds of intermolecular H-bonding involving in N–H stretching may exist in PMMA: firstly the intermolecular H-bonding between amide N–H and C=O in $\mathbf{II_b}$, and between amide N–H in $\mathbf{II_b}$ and C=O in PMMA. As shown in Fig. 1B, the spectrum of $\mathbf{II_b}$ in KBr exhibited IR bands corresponding to C=O stretching vibration at 1674 and 1682 cm^{-1} and N–H stretching vibration at 3420 cm^{-1}. However, when $\mathbf{II_b}$ was doped into PMMA, the C=O stretch band shifted to 1670 cm^{-1}, the N–H stretch band to 3377 cm^{-1} and the amide N–H deformation band appeared at 1535 cm^{-1}. The strong band at ~1730 cm^{-1} was attributed to the C=O stretching vibration band of PMMA. The H-bonding can also be verified by the shifted bands at 1700 cm^{-1} for C=O stretch and 3329 cm^{-1} for N–H···O (THF) stretch vibration in THF solution of $\mathbf{II_b}$. Consequently, the amide N–H in $\mathbf{II_b}$ forms an intermolecular H-bonding with C=O in other azobenzenes but not in the PMMA polymer chain, which is represented in Scheme 2.

3.2. UV–vis spectra

The UV–vis spectra of $\mathbf{I_b}$ and $\mathbf{II_b}$ in PMMA film and $CHCl_3$ solution are shown in Fig. 2. The photophysical properties of $\mathbf{I_{a-c}}$ and $\mathbf{II_{a-c}}$ are summarized in Table 1. The maximum absorption peak of $\mathbf{II_b}$ near 361 nm is assigned to the π–π* transition for the *trans* isomer. The direction of the π–π* transition moment of the *trans* form is known to align with the long axis. An absorption maximum of $\mathbf{I_b}$ appears at 376 nm and shows a 15-nm redshift compared with that of $\mathbf{II_b}$ due to the stronger electron-donating ability of amino group than the acetylamino group. The absorption maximum of $\mathbf{I_a}$ exhibits an approximately 5-nm blueshift compared to $\mathbf{I_{b-c}}$, which might be due to the electron-donating ability of the alkyl group.

The absorption maxima of azobenzenes $\mathbf{I_{a-c}}$ exhibited systematic redshifts 11.6–14.6 nm in the PMMA films compared to those in solution. A slight broadening of this band was also observed. The broadening and redshift of the absorption band can be assigned to the development of a local internal electric field caused by parallel dipole alignment [20,21]. The absorption maxima of $\mathbf{II_{a-c}}$ in PMMA film only shifted about 4.0–6.8 nm comparing to those in solution, which were smaller than those for $\mathbf{I_{a-c}}$. As shown in Fig. 2, the absorption spectra of $\mathbf{II_b}$ in the PMMA films showed a maximum at 365.8 nm and a clear shoulder peak at 380 nm. These may be due to the aggregation of aminoazobenzene $\mathbf{II_b}$ in PMMA formed by the intermolecular H-bonding between the amide groups in $\mathbf{II_b}$ as mentioned above.

3.3. Photoisomerization

The dependence of irradiation power on the absorbance of azobenzene was investigated. A linear dependence on the irradiation power was obtained between 1 mW and 7 mW (Fig. 3). In order to avoid the destruction of azobenzenes, laser power of 3 mW was chosen for the subsequent experiments.

All absorption spectra of azobenzene-doped PMMA films were recorded by varying irradiation time. As an example the spectral variation for $\mathbf{I_{a-c}}$ is shown in Fig. 4. With increasing irradiation time, the *trans* isomer absorption (about 385 nm) decreases sharply together with the increase in the *cis* isomer absorption (near 500 nm). The absorption changes very fast at first and the rate becomes very slow after 7 min indicating that the

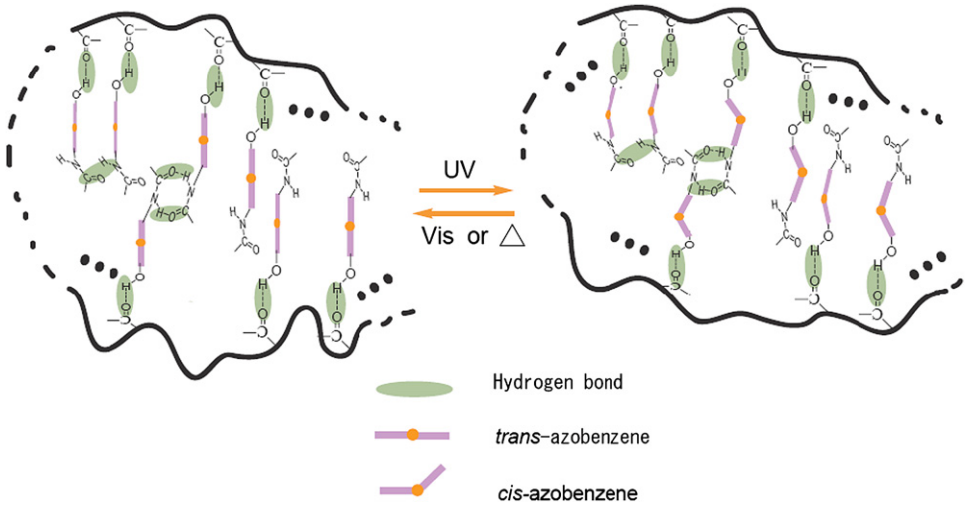

Scheme 2. The concept of intermolecular hydrogen bonding of $\mathbf{II_{a-c}}$ in PMMA matrix.

equilibrium was reached. For $\mathbf{II_a}$, the absorption was reduced to 45% of its initial value, which is a more significant change than $\mathbf{I_a}$. It also took a longer time (12 min) to reach equilibrium (Fig. 4).

4. Discussion

4.1. Dynamics

The predominant photochemistry of azobenzenes involves reversible photoisomerization from a thermally stable *trans* form to a *cis* form; the backward reaction can occur both photochemically and thermally (Eq. (1)). When the forward and backward reaction rates are equal, the system reaches a photostationary state at equilibrium.

$$trans \underset{k_{-1}(h\nu',\Delta)}{\overset{k_1(h\nu)}{\rightleftharpoons}} cis \tag{1}$$

According to the dynamics function the integrated rate constant for approach to the equilibrium is given by Eq. (2).

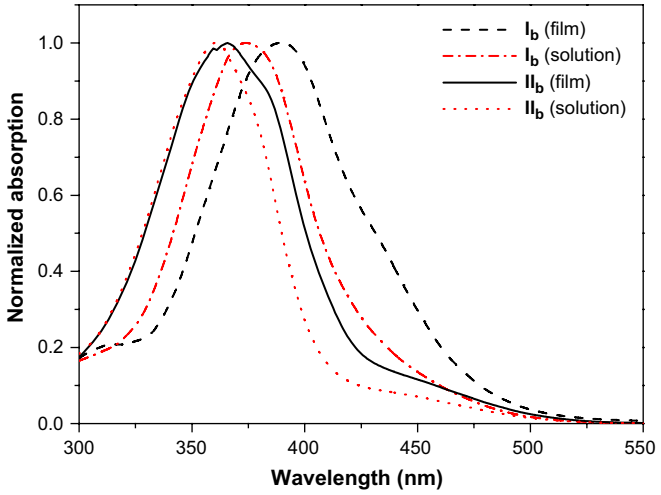

Fig. 2. The normalized UV–vis spectra of $\mathbf{I_b}$ in film (dash) and solution (dash dot), and $\mathbf{II_b}$ in film (solid) and solution (dot).

$$[trans]_t = [trans]_e + \left([trans]_0 - [trans]_e\right)e^{(-kt)} \tag{2}$$

where $[trans]_0$, $[trans]_e$, $[trans]_t$ are the concentrations of the *trans* form in the initial condition, at equilibrium, and at time t, respectively. The rate constant k is the sum of rate constants for forward and reverse reactions.

It is assumed that only *trans* form exists in doped polymer before irradiation. The concentration of *trans* form ($[trans]_t$) isomers can be calculated from the absorbance at different irradiation times according to Eq. (3). Consequently the integrated rate constant can be calculated according to the absorption spectra and Eq. (4).

$$[trans]_t = \frac{A_t}{A_0} \tag{3}$$

$$A_t = A_e + (1 - A_e)e^{(-kt)} \tag{4}$$

where A_0, A_t and A_e are the absorbance of the *trans* form at start, at time t and at the equilibrium.

4.2. Substituent effect

In studying the effect of substituents, the 4-substituents varied from hydroxyl (**a**), hydroxypropoxy (**b**) to hydrohexyloxy (**c**), and the 4′-substituents varied from amino (**I**) to acetylamino

Table 1
The photophysical properties of azobenzene dyes in solution and in film

Dye	λ_{max}^{sol} [a] (nm)	ε_{max} [b] ($M^{-1}\,cm^{-1}$)	λ_{max}^{film} [c] (nm)	$\Delta\lambda$ [d]
$\mathbf{I_a}$	371.2	26 000	385.8	14.6
$\mathbf{I_b}$	376.4	26 900	388.0	11.6
$\mathbf{I_c}$	377.4	25 200	389.2	11.8
$\mathbf{II_a}$	358.2	30 200	365.0	6.8
$\mathbf{II_b}$	361.4	19 800	365.8	4.4
$\mathbf{II_c}$	362.0	19 100	366.0	4.0

[a] The absorption maximum of azobenzenes at a concentration of 5.0×10^{-5} M in chloroform.
[b] Molar coefficient of azobenzenes in chloroform.
[c] The absorption maximum of azobenzenes in film.
[d] $\Delta\lambda = \lambda_{max}^{film} - \lambda_{max}^{sol}$.

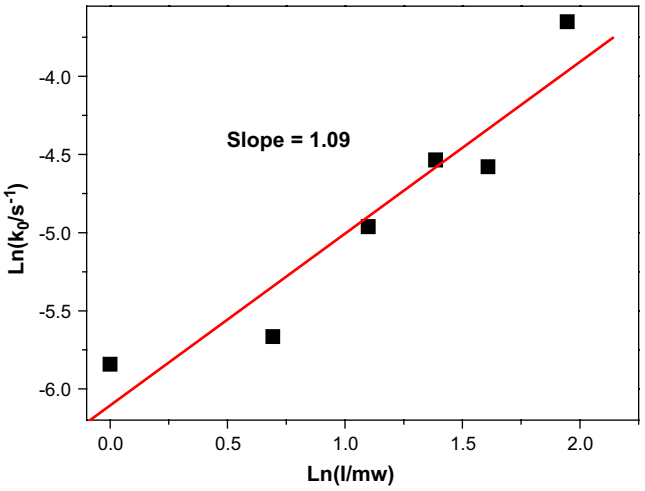

Fig. 3. Dependence of the initial rate for **II**$_b$ on the laser power at 355 nm. The solid line is the fitting line ($r = 0.95$).

(**II**). As mentioned above, intermolecular H-bonding exists between two acetylamino groups in compounds **II**$_{a–c}$ (Scheme 2), which may affect the photochemical behavior.

The ratios of *trans* isomers with increasing irradiation time were investigated for **I**$_{a–c}$ and **II**$_{a–c}$. As shown in Figs. 4d and 5d, the decreased rate of *trans*-form ratio ranked in the order of **c** > **a** > **b** when the spacer length at the 4-position varied with methylene numbers $(CH_2)_n$ where n = 0 for **a**, 3 for **b** and 6 for **c**, respectively. The rate constants were calculated according to Eq. (4) and all of the data are summarized in Table 2. When the spacer length is shorter than three methylenes, the larger substituent restricts the motion of the chromophores comparing **I**$_a$ with **I**$_b$ and **II**$_a$ with **II**$_b$. Here, a lower rate constant of photoisomerization was observed. When the spacer length is increased to six methylenes, the free volume in the polymer is increased. Therefore, the motions of **I**$_c$ and **II**$_c$ are increased. Compound **I**$_c$ possessed the highest rate constant in series **I**, as did **II**$_c$ in series **II**.

When the 4′-substituents were changed from amino (**I**$_{a–c}$) to acetylamino (**II**$_{a–c}$), the concentrations of *cis* form at equilibrium for **II**$_{a–c}$ were 49–60%, much higher than those for **I**$_{a–c}$ (about 35%). The rate constants for the backward reaction *cis* → *trans* for **II**$_{a–c}$ were 3–5 times smaller than those for **I**$_{a–c}$ (Table 2). One possible reason is the steric limitation of the substituent was increased, and the free volume for isomerization in the polymer matrix was decreased. Another possibility is the existence of intermolecular H-bonding between molecules of **II**$_{a–c}$ making the azo dyes aggregate, so their photoisomerization should be significantly reduced, compared to **I**$_{a–c}$. These intermolecular H-bondings restrain the backward reaction *cis* → *trans* and influence the final ratio of *cis* form at equilibrium. Although azo dyes with a blue-shifted spectrum have a longer *cis* lifetime [14], here the longer lifetimes of the *cis* form of **II**$_{a–c}$ are mainly due to an intermolecular H-bonding effect.

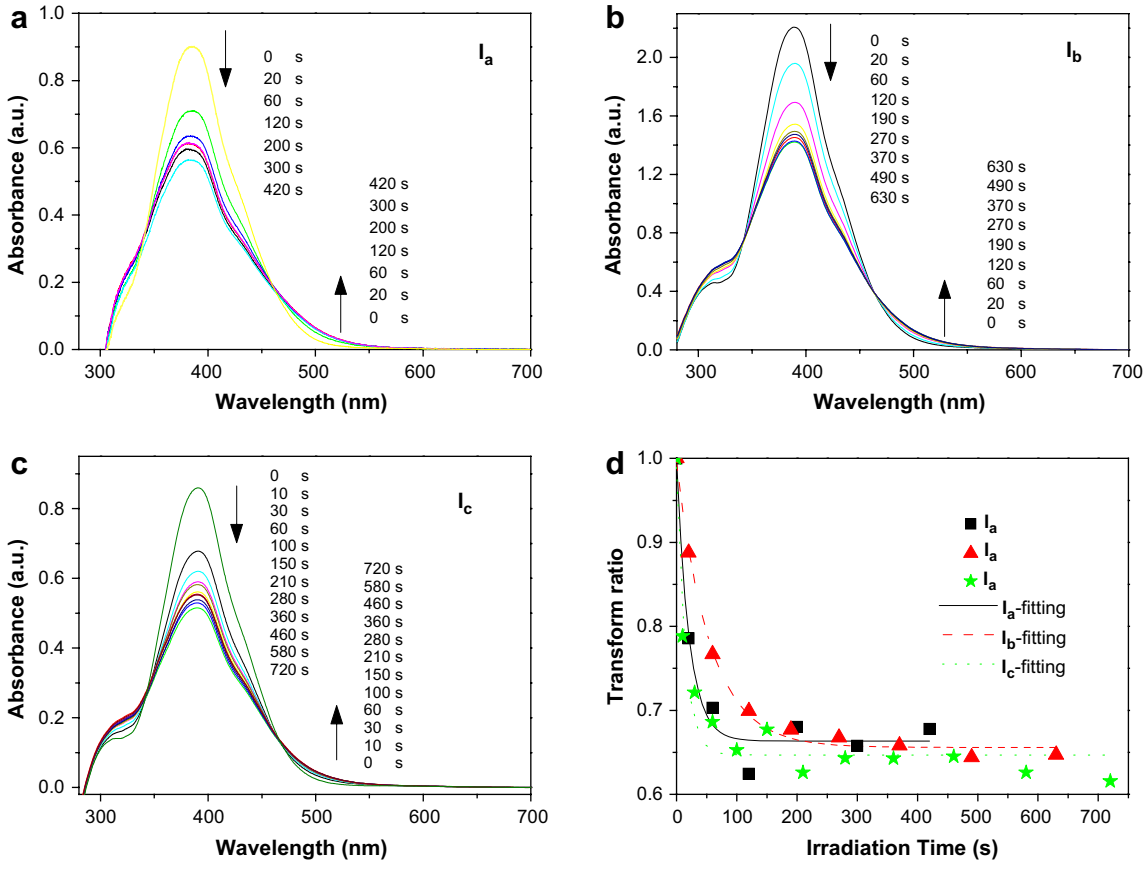

Fig. 4. The photoisomerization of compounds **I**$_a$ (a), **I**$_b$ (b) and **I**$_c$ (c) with increasing irradiation time at 355 nm with light power of 3.0 mW (10 wt% doped in PMMA film). (d) The ratio of the *trans* isomer with increasing irradiation time.

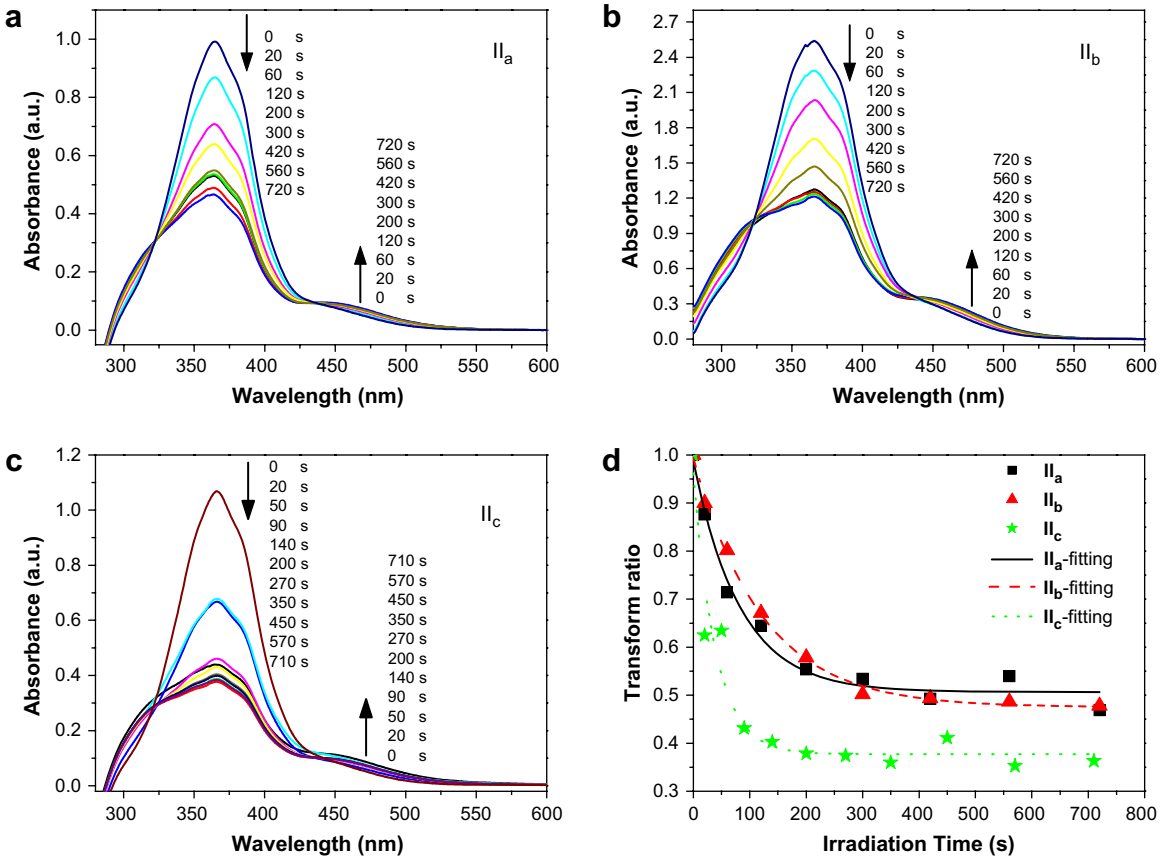

Fig. 5. The photoisomerization of compounds $\mathbf{II_a}$ (a), $\mathbf{II_b}$ (b) and $\mathbf{II_c}$ (c) with increasing irradiation time at 355 nm with light power of 3.0 mW (10 wt% doped in PMMA film). (d) The ratio of the *trans* isomer with increasing irradiation time.

To this point, compounds $\mathbf{II_{a-c}}$ are good candidates for development of high-speed actuators for microscale or nanoscale applications, for example the micro-robots proposed for use in medicine and for optically actuated microtweezers.

4.3. Concentration effect

The photoisomerization behavior of compounds $\mathbf{I_b}$ and $\mathbf{II_b}$ was investigated by varying doping concentration in PMMA.

Table 2
The rate constants of azo dyes in PMMA under irradiation with laser power of 3 mW

Dye	Concentration (wt%)	k_1[a] (10^{-2} s^{-1})	k_1[b] (10^{-2} s^{-1})	k_1[c] (10^{-2} s^{-1})	[*trans*][d] (%)	[*cis*][d] (%)
$\mathbf{I_a}$	10	1.601	3.154	4.755	66.3	33.7
$\mathbf{I_b}$	2	0.391	1.326	1.717	76.7	23.3
	5	1.423	2.078	3.501	59.4	40.6
	10	0.623	1.189	1.812	65.6	34.4
$\mathbf{I_c}$	10	2.434	4.467	6.901	64.7	35.3
$\mathbf{II_a}$	10	0.597	0.613	1.210	50.6	49.4
$\mathbf{II_b}$	2	0.990	0.489	1.479	33.0	67.0
	5	1.227	0.743	1.970	37.7	62.3
	10	0.432	0.391	0.823	44.3	55.7
$\mathbf{II_c}$	10	1.573	0.952	2.525	37.7	62.3

[a] Rate constant from *trans* to *cis*.
[b] Rate constant from *cis* to *trans*.
[c] The integrate rate constant ($k_1 + k_{-1}$).
[d] The equilibrium ratio in film after irradiation.

We found that the rate constant of $\mathbf{I_b}$ and $\mathbf{II_b}$ increased when the doping concentration increased from 2% to 5%. However, the rate constant increased from 1.81×10^{-2} s^{-1} to 3.50×10^{-2} s^{-1}, when the doping concentration decreased from 10% to 5% for compound $\mathbf{I_b}$. A similar result was observed for $\mathbf{II_b}$, where the rate constant varied from 0.82×10^{-2} s^{-1} to 1.97×10^{-2} s^{-1} with the concentration decreasing from 10% to 5% (Table 2). Since intermolecular H-bondings exist between hydroxyl groups in $\mathbf{I_{a-c}}$ (or $\mathbf{II_{a-c}}$) and carbonyl group in the PMMA polymer, azobenzenes ($\mathbf{I_{a-c}}$ and $\mathbf{II_{a-c}}$) may be anchoring on the PMMA chain, where their rotational motion would be restricted by the free volume in the PMMA. When azobenzenes doped in PMMA reach a certain concentration, their free rotational motion would be restricted by potential aggregation within a reduced free volume. Therefore, the abnormally decreased rate constants were observed when the concentrations of $\mathbf{I_b}$ and $\mathbf{II_b}$ increased from 5% to 10%.

5. Conclusion

Two series of azobenzenes were synthesized and their photoisomerization behaviors in the polymer matrix (PMMA) were investigated by UV–vis spectra. The rate constants were calculated according to dynamics equations for reversible photoisomerization. Aminoazobenzenes $\mathbf{I_{a-c}}$ exhibited faster photoisomerization and had larger integration rate constants

than the corresponding acetylamino derivatives $\mathbf{II_{a-c}}$. Azobenzenes with a longer alkyl chain ($\mathbf{I_c}$, $\mathbf{II_c}$) showed a faster photoisomerization rate than those with shorter chains ($\mathbf{I_b}$, $\mathbf{II_b}$). At equilibrium, *cis* ratios of $\mathbf{II_{a-c}}$ (49–60%) were higher than those of $\mathbf{I_{a-c}}$ (35%) due to larger steric limitation and intermolecular hydrogen bonding interactions between acetylamino groups.

Acknowledgements

We acknowledge financial support from ''One Hundred Oversea Talent'' program of Chinese Academy of Sciences (CAS) and CREST program, Japan Science and Technology Agency (JST).

References

[1] Natansohn A, Rochon P, Gosselin J, Xie S. Azo polymers for reversible optical storage. 1. Poly[4′-[[2-(acryloyloxy)ethyl]ethylamino]-4-nitroazobenzene]. Macromolecules 1992;25:2268–73.

[2] Ikeda T, Tsutsumi O. Optical switching and image storage by means of azobenzene liquid-crystal films. Science 1995;268:1873–5.

[3] Kim DY, Tripathy SK, Li L, Kumar J. Laser-induced holographic surface relief gratings on nonlinear optical polymer films. Applied Physics Letters 1995;66:1166–8.

[4] Rochon P, Batalla E, Natansohn A. Optically induced surface gratings on azoaromatic polymer films. Applied Physics Letters 1995;66:136–8.

[5] Bŭchel M, Sekkat Z, Paul S, Weichart B, Menzel H, Knoll W. Langmuir–Blodgett–Kuhn multilayers of polyglutamates with azobenzene moieties: investigations of photoinduced changes in the optical properties and structure of the films. Langmuir 1995;11:4460–6.

[6] Branger C, Lequan M, Lequan RM, Large M, Kajzar F. Polyurethanes containing boron chromophores as sidechains for nonlinear optics. Chemical Physics Letters 1997;272:265–70.

[7] Kang HC, Lee BM, Yoon J, Yoon M. Synthesis and surface-active properties of new photosensitive surfactants containing the azobenzene group. Journal of Colloid and Interface Science 2000;231:255–64.

[8] Haitjema HJ, von Morgan GL, Tan YY, Challa G. Photoresponsive behavior of azobenzene-based (meth)acrylic (*co*)polymers in thin films. Macromolecules 1994;27:6201–6.

[9] Sekkat Z, Knoll W. Photoreactive organic thin films. Academic Press; 2002.

[10] Ho MS, Natansohn A, Rochon P. Azo polymers for reversible optical storage. 7. The effect of the size of the photochromic groups. Macromolecules 1995;28:6124–7.

[11] Magennis SW, Mackay FS, Jones AC, Tait KM, Sadler PJ. Two-photon-induced photoisomerization of an azo dye. Chemistry of Materials 2005;17:2059–62.

[12] Chen JP, Lagugné LF, Natansohn A, Rochon P. Highly stable optically induced birefringence and holographic surface gratings on a new azocarbazole-based polyimide. Macromolecules 1999;32:8572–9.

[13] Meng X, Natansohn A, Rochon P. Azo polymers for reversible optical storage: 13. Photoorientation of rigid side groups containing two azo bonds. Polymer 1997;38:2677–82.

[14] Natansohn A, Rochon P. Photoinduced motions in azo-containing polymers. Chemical Reviews 2002;102:4139–75.

[15] Pajak J, Rospenk M, Sobczyk L. Liquid crystalline properties and IR spectra of 2′-hydroxy-4′-octyloxyazobenzenes. Spectrochimica Acta A 2003;59:2131–40.

[16] Yager Kevin G, Barrett Christopher J. Novel photo-switching using azobenzene functional materials. Journal of Photochemistry and Photobiology A: Chemistry 2006;182:250–61.

[17] Ruggli P, Petitjean C. Über poly-azobenzole. Helvetica Chimica Acta 1938;21:711–20.

[18] Angeloni AS, Caretti D, Carlini C, Chilellini E, Galli G, Altomare A, et al. Photochromic liquid-crystalline polymers. Main chain and side chain polymers containing azobenzene mesogens. Liquid Crystals 1989;4:513–27.

[19] Chen WQ, Ya Q, Duan XM. *N*-(4-Hydroxyphenyl)acrylamide. Acta Crystallographica Section E 2006;E62:o145–6.

[20] Wedel A, Strohriegl P, Danz R. In-situ absorption studies of nonlinear optically active side-chain polymers during corona poling. Acta Polymerica 1993;44:302–6.

[21] Tsutsumi N, Ono T, Kiyotsukuri T. Internal electric field and second harmonic generation in the blends of vinylidene fluoride–trifluoroethylene copolymer and poly(methyl methacrylate) with a pendant nonlinear optical dye. Macromolecules 1993;26:5447–56.